Research paper

Physiological characteristics and RNA sequencing in two root zones with contrasting nitrate assimilation of *Populus × canescens*

Jing Zhou, Yan Lu, Wen-Guang Shi, Shu-Rong Deng and Zhi-Bin Luo[1,2]

[1]State Key Laboratory of Tree Genetics and Breeding, Key Laboratory of Silviculture of the National Forestry and Grassland Administration, Research Institute of Forestry, Chinese Academy of Forestry, Beijing 100091, China; [2]Corresponding author (luozbbill@163.com)

Different root zones have distinct capacities for nitrate (NO$_3^-$) uptake in *Populus* species, but the underlying physiological and microRNA (miRNA) regulatory mechanisms remain largely unknown. To address this question, two root zones of *Populus × canescens* (Ait.) Smith. with contrasting capacities for NO$_3^-$ uptake were investigated. The region of 0–40 mm (root zone I) to the root apex displayed net influxes, whereas the region of 40–80 mm (root zone II) exhibited net effluxes. Concentrations of NO$_3^-$ and ammonium (NH$_4^+$) as well as nitrate reductase activity were lower in zone II than in zone I. Forty one upregulated and twenty three downregulated miRNAs, and 576 targets of these miRNAs were identified in zone II in comparison with zone I. Particularly, *growth-regulating factor 4 (GRF4)*, a target of upregulated ptc-miR396g-5p and ptc-miR396f_L + 1R-1, was downregulated in zone II in comparison with zone I, probably contributing to lower NO$_3^-$ uptake rates and assimilation in zone II. Furthermore, several miRNAs and their targets, members of *C2H2* zinc finger family and *APETALA2*/ethylene-responsive element binding protein family, were found in root zones, which probably play important roles in regulating NO$_3^-$ uptake. These results indicate that differentially expressed miRNA–target pairs play key roles in regulation of distinct NO$_3^-$ uptake rates and assimilation in different root zones of poplars.

Keywords: miRNAs, net NO$_3^-$ flux, nitrate, poplar, root zones.

Introduction

Nitrogen (N) is one of the most important macronutrients and is essential for plant growth and development. Indeed, N accounts for 1.5–2.0% of plant dry matter and is a component of many biomolecules, including proteins and nucleic acids (Zhang et al. 2016, Kant 2018). Nitrate (NO$_3^-$) is the primary form of inorganic N acquired from soil by plant roots. However, NO$_3^-$ concentrations vary widely in soil solutions, typically in the range of 0.5–10 mM (Miller et al. 2007). In general, the plant–root system exhibits high plasticity, allowing adaptation to fluctuations in soil NO$_3^-$ concentrations (Sorgonà et al. 2010, Kant 2018, Ruan et al. 2019). For example, compared with 1 mM ammonium (NH$_4^+$), 1 mM NO$_3^-$ can promote primary

root growth in *Arabidopsis thaliana* Heynh. (Liu et al. 2013) and *Populus simonii × P. nigra* T. S. Hwang et Liang (Qu et al. 2016), whereas *A. thaliana* lateral root development is inhibited by 5 mM NO$_3^-$ compared with 0.5 mM NH$_4^+$ (Gifford et al. 2008). Despite much research progress on the effect of NO$_3^-$ on root morphological characteristics (Remans et al. 2006, Liu et al. 2013, Qu et al. 2016), limited information is available about the effect of NO$_3^-$ on different root zones of plants and their internal regulatory characteristics.

The uptake rate of NO$_3^-$ is spatially variable along the roots of different plants (Henriksen et al. 1990, Cruz et al. 1995, Colmer and Bloom 1998, Taylor and Bloom 1998, Luo et al.

2013b). For instance, the net flux of NO_3^- appears to be low near the apex and high in the basal zones of both barley (Henriksen et al. 1990) and maize roots (Taylor and Bloom 1998). However, the opposite pattern has been reported for rice and carob roots (Cruz et al. 1995, Colmer and Bloom 1998). Moreover, for the same plant, the net NO_3^- fluxes in different root zones can vary spatially (Luo et al. 2013b, Zhang et al. 2014, Zhong et al. 2014). Plants have evolved highly flexible and dynamic transport systems to cope with changes in net NO_3^- fluxes in different root zones (Selle et al. 2005, Sorgona et al. 2011, Alber et al. 2012, Lupini et al. 2016). For instance, a significant correlation ($P = 0.0023$) was observed between NO_3^- influx and gene transcript levels in maize (*Zea mays* Linnaeus) roots, but only when *NAR2.1* and *NRT2.1* co-expression was considered under NO_3^- conditions (Lupini et al. 2016). These studies provide evidence that different root zones of the same plant display different net NO_3^- fluxes, which are correlated with the transcript levels of relevant genes (Sorgona et al. 2011, Alber et al. 2012, Zhong et al. 2014, Lupini et al. 2016). Although many studies have reported the influxes and effluxes of NO_3^- in different root zones, the underlying physiological and microRNAs (miRNAs) regulatory mechanisms have not yet been elucidated.

miRNAs are non-coding small RNAs (sRNAs) with a length of ~18–25 nucleotides (nts). miRNAs inhibit gene expression at the post-transcriptional level by promoting cleavage or suppressing the translation of target genes, affecting plant growth, development and adaptation to changing environments (Tang et al. 2003, Sunkar et al. 2012, Zhou et al. 2012, Ren et al. 2015, Yu et al. 2018). In recent years, many miRNAs and their target genes have been identified to be associated with NO_3^- uptake and assimilation in the roots of model plants (Li et al. 2016, Zuluaga et al. 2017, Jiang et al. 2018, Yu et al. 2018). As an example, miR167 expression was repressed by 5 mM NO_3^- in the pericycle cells of *Arabidopsis* roots, and the expression level of its target *AUXIN RESPONSE FACTOR 8* (*ARF8*) was increased to promote lateral root initiation and emergence (Gifford et al. 2008, Gutierrez 2012). This finding indicates that miR167-*ARF8* can respond to NO_3^- influx by inducing changes in root structure (Gifford et al. 2008, Gutierrez 2012). Previous studies have also demonstrated that miRNAs are regulated by NO_3^- to further modulate target genes and affect the uptake and assimilation of NO_3^- in plants (Gifford et al. 2008, Vidal et al. 2010, Gutierrez 2012). However, no information is currently available on miRNAs regulatory mechanisms underlying NO_3^- uptake and assimilation in different root zones.

As a fast-growing woody plant, poplar species require a large amount of N fertilizers to support rapid growth and development (Zhang et al. 2014). Most poplar species prefer to absorb NO_3^- (Rennenberg et al. 2010, Rewald et al. 2016, Zhang et al. 2016). Moreover, NO_3^- fluxes were spatially variable along the root tips of *P. popularis* (Luo et al. 2013b). Nevertheless,

it remains unknown how miRNAs affect net NO_3^- fluxes in different root zones of poplar. Thus, it is of great importance for us to elucidate the physiological and molecular regulatory mechanisms underlying the distinct capacities for NO_3^- uptake and assimilation in different root zones of poplar.

In this study, *Populus* × *canescens* (synonym: *Populus tremula* × *Populus alba* 717-1B4) saplings were cultivated with 500 μM $NaNO_3$ for 10 days. The aims of this study were (i) to identify root zones with contrasting NO_3^- uptake rates and N assimilation and (ii) to dissect the miRNA regulatory mechanisms underlying the distinct characteristics of NO_3^- uptake and assimilation in the root zones of *P.* × *canescens*. To achieve these aims, net NO_3^- fluxes along root tips were measured, and physiological parameters (e.g., concentrations of NO_3^- and NH_4^+, and activities of nitrate reductase (NR), glutamine synthetase (GS) and glutamate synthase (GOGAT)) in the different root zones were assessed. The results showed that poplar root tips can be divided into two zones with significant differences in NO_3^- uptake rates and assimilation. We also characterized the expression profiles of miRNAs and their targets in the two root zones by RNA sequencing. The results of this study provide new insights into the physiological and miRNAs regulatory mechanisms underlying contrasting net NO_3^- fluxes in distinct root zones of poplars.

Materials and methods

Plant cultivation

Plantlets of *P.* × *canescens* (*P. tremula* × *P. alba*, INRA 717-IB4 clone) were obtained through micropropagation and cultivated in a climate chamber (light per day: 16 h; photosynthetic photon flux density: 150 μmol m^{-2} s^{-1}; day/night temperature: 25/20 °C; relative humidity: 50–55%) for 1 month. The plants were then transferred to plastic pots (10 L) filled with fine sand and cultivated in a growth room under conditions similar to those in the climate chamber. Each plant was supplied with 50 ml of modified Long Ashton (LA) solution (Dluzniewska et al. 2007, 500 μM NH_4NO_3, 0.5 mM KCl, 0.9 mM $CaCl_2$, 0.3 mM $MgSO_4$, 0.6 mM KH_2PO_4, 42 μM K_2HPO_4, 10 μM Fe-EDTA, 2 μM $MnSO_4$, 10 μM H_3BO_3, 7 μM Na_2MoO_4, 0.05 μM $CoSO_4$, 0.2 μM $ZnSO_4$ and 0.2 μM $CuSO_4$) every other day for 2 weeks. Subsequently, the plants were transferred to a hydroponic system with LA nutrients and grown for 14 days. Before harvest, the plants were cultivated in modified LA solution with 500 μM NH_4NO_3 replaced by 500 μM $NaNO_3$ for 10 days. Fifty-four plants with similar growth performance were used for further experiments.

Analysis of net NO_3^- fluxes

The method of measuring net NO_3^- fluxes along the root tips of *P.* × *canescens* was based on the description of Luo et al. (2013b). To determine the major region of NO_3^- influx/efflux

along the poplar root tip, a preliminary experiment was carried out with an initial measurement at the root tip followed by measurements every 5 mm (in the region of 0–80 mm). To measure net NO_3^- fluxes in the *P. × canescens* root, one white fine root was excised from the root system of each plant, and net NO_3^- fluxes were measured in a 500 μM $NaNO_3$ solution using a non-invasive micro-test technique (BIO-001A3 system; Younger USA Science and Technology Corp., Applicable Electronics Inc., Science Wares Inc., Falmouth, MA, USA). NO_3^- fluxes were recorded at each measurement point for 5 min, and six plants were used for this analysis.

Harvesting

The root system of each *P. × canescens* plant was carefully washed with the modified LA solution (containing 500 μM $NaNO_3$ instead of 500 μM NH_4NO_3), and the root tips were divided into zones I and II according to the spatial patterns of net NO_3^- fluxes. The root samples were wrapped with tin foil and immediately frozen in liquid N. The root samples were ground into fine powder in liquid N using a mortar and pestle and stored at −80 °C for further physiological and molecular analyses. To obtain enough material for analysis, equal amounts of fine power from the same root zone samples of eight plants were pooled and mixed well. Therefore, six pooled samples were obtained.

Determination of NO_3^- and NH_4^+ concentrations, and enzymatic activities

Nitrate concentrations in the two root zones were analyzed spectrophotometrically, according to Patterson et al. (2010), and NH_4^+ concentrations in the two root zones were determined based on the Berthelot reaction (Luo et al. 2013b). Activities of NR (EC 1.7.99.4), glutamine synthetase (GS, EC 6.3.1.2) and glutamate synthase (GOGAT, EC 1.4.7.1) in the two root zones were assayed according to the methods described in our previous study (Luo et al. 2013a).

Construction of sRNA libraries for high-throughput sequencing

Total RNA was extracted from the samples using a total RNA kit (TRK1001, LianChuan (LC) Science, Hangzhou, China) following the manufacturer's protocol and then assessed for quality using a NanoDrop 2000 spectrophotometer (Thermo, Wilmington, DE, USA) at 260/280 nm (ratio >2.0). Three cDNA libraries from each root zone were prepared and sequenced by LC Sciences using the Illumina HiSeqTM2500 platform (Hangzhou, China).

Small RNA data analysis and identification of known and novel miRNAs

After sequencing, raw data from Illumina sequencing were further analyzed using the ACGT101-miR program (LC Sciences, Houston, TX, USA). The raw data were first cleaned by removing low quality tags and sequences (i.e., sequences of <19 nts or >25 nts). The remaining clean and unique reads were subjected to a further filtration step, to remove common RNA families (ribosomal RNA (rRNA), transfer RNA (tRNA) and small nuclear RNA (snRNA)), and the remaining clean and unique reads were aligned to sequences from the miRBase database (version 21.0, http://www.mirbase.org/). Because the stem–loop hairpin structure is an important indicator of a miRNA, secondary structures were predicted using RNAfold software (http://rna.tbi.univie.ac.at/cgi-bin/RNAfold.cgi), as suggested by Griffiths-Jones et al. (2008). The miRNAs from the plants that matched those in the miRBase database and with stable hairpin structures were classified as known miRNAs. In addition, pre-miRNAs with a stable hairpin structure and a minimal folding free energy index >0.9 were considered as novel miRNAs in this study. All of the sequencing data, including sRNA sequences and transcriptomic sequences, were deposited in the National Center for Biotechnology Information Sequence Read Archive database under accession number PRJNA533725 (https://www.ncbi.nlm.nih.gov/bioproject/PRJNA533725).

For each sample, the frequency of the miRNAs was normalized by Z-score transformation. Fold changes in differentially expressed miRNAs were determined by the ratio of the Z-score in root zone II compared with that in root zone I. Significantly differentially expressed miRNAs were identified by P-values <0.05. A heatmap of the significantly differentially expressed miRNAs was constructed using Cytoscape software (3.5.1).

Target identification and analysis

Target genes of the miRNAs were predicted using the TargetFinder web server (https://github.com/carringtonlab/TargetFinder) according to a previously described method (Allen et al. 2005). A penalty score (alignment score) criterion was introduced based on the alignment between each miRNA and its potential target. Mismatched pairs were scored as 1, and G/U pairs were scored as 0.5. Counting from the 5′ end of the miRNA sequence, the score was doubled for mismatches located between the second base and the 13th base inclusive. A transcript with total scores (including mismatches and G/U pairs) <4 in complementary regions was regarded as a miRNA target.

To measure the expression profiles of target genes, three independent cDNA libraries were constructed using RNA samples from root zones I to II, respectively, and subjected to transcriptomic sequencing. For each library, all of the sequences were processed to filter out adaptor sequences and low-quality sequences. Next, all of the clean tags were mapped to the assembled unigenes of *P. × canescens* for annotation, and the TargetFinder results were mapped against the *P. × canescens* transcriptomic data. The target genes in *Populus trichocarpa* were submitted to MapMan for functional category analysis, as described by Jia et al. (2017).

Combining TargetFinder results and transcriptomic sequencing, the fragments per kilobase of exon per million fragments mapped (FPKM) algorithm was used to calculate the level of target gene expression (Pertea et al. 2015). Fold changes in differentially expressed target genes were determined using the FPKMs of genes in root zone II compared with those in root zone I. Significantly differentially expressed target genes between root zones II and I were identified by the following conditions: absolute values of fold changes >2 and P-values <0.05.

Validation of significantly differentially expressed miRNAs and genes by quantitative RT-PCR

To validate the identified significantly differentially expressed miRNAs and target genes, qRT-PCR analysis was performed using SYBR Green detection reagents (Quanta Biosciences, USA) with a LightCycler® 480 RealTime PCR System (Roche, USA), as reported by Zhou et al. (2012). Nine differentially expressed miRNA-target pairs were validated by qRT-PCR analysis. The expression levels of several genes encoding NO_3^- transporters and enzymes involved in N assimilation were also analyzed. The RNA samples used for qRT-PCR analysis were the same as those used for the sequencing described above. Specific primers for mature miRNAs and their predicted target genes were designed (Table S1 available as Supplementary Data at Tree Physiology Online). U6 and ACTIN2/7 were selected as reference genes for the validation of miRNAs and target genes, respectively (Zhou et al. 2012).

Validation of miRNA-target pairs

To validate the miRNA-target pairs, transient co-expression assays were carried out using Nicotiana benthamiana leaves according to the methods of Cao et al. (2016) and Wu et al. (2013). Two miRNA-target pairs were chosen. Briefly, genomic fragments forming fold-back structures coding for precursors of miRNAs were amplified using genomic DNA from root samples and sequence-specific primers (Table S1 available as Supplementary Data at Tree Physiology Online). Similarly, fragments of the target genes harboring miRNA complementary sites were amplified using total RNA isolated from root samples and specific primers (Table S1 available as Supplementary Data at Tree Physiology Online). The miRNAs and target genes were cloned into the pCAMBIA2300 and pCAMBIA1300 vectors, respectively, both of which carry a 35S promoter. Subsequently, the constructs harboring the cloned miRNAs and target genes were transformed into Agrobacterium tumefaciens strain GV3101 by electroporation. Equal amounts of agrobacterial cell cultures containing miRNAs and their corresponding target genes were mixed and infiltrated into N. benthamiana leaves as described previously (He et al. 2008). Leaves were harvested 2 days after infiltration for qRT-PCR analysis with gene specific primers (Table S1 available as Supplementary Data at Tree Physiology Online). Two genes, tobacco 5.8S RNA and tubulin (Table S1), were selected as reference genes for validation of the miRNAs and target genes, respectively.

Statistical analysis

Net NO_3^- flux data were calculated and exported with Mage Flux software (version 1.0) attached to a non-invasive micro-test technique system (Xu et al. 2006). The data were tested for normality prior to the statistical analysis. One-way analysis of variance (ANOVA) was performed with the distance from the root apex as a factor. The data for NO_3^- and NH_4^+ concentrations and enzymatic activities were also tested for normality prior to statistical analysis using ANOVA, with the root zones as a factor. Differences between means were considered significant when $P < 0.05$ according to the ANOVA F-test. The Ct values obtained from qRT-PCR were normalized, and the relative fold changes in miRNAs and their target genes were calculated (Pfaffl et al. 2002).

Results

Net NO_3^- fluxes along poplar root tips

To investigate spatial variations in NO_3^- absorption along the roots of P. × canescens, net NO_3^- fluxes were monitored along the root tips from the apex to the base for a total length of ∼80 mm (Figure 1a). Net fluxes along the root axis varied from 42.8 (influx) to −13.4 pmol cm^{-2} s^{-1} (efflux, Figure 1b), and the poplar root tip was therefore divided into zone I (0–40 mm) and zone II (40–80 mm). Root zone I displayed net influxes with an average of 18.5 pmol cm^{-2} s^{-1}. In contrast, root zone II showed net effluxes with a mean rate of −8.0 pmol cm^{-2} s^{-1} (Figure 1c).

Nitrate and NH_4^+ concentrations and enzymatic activities

As different net NO_3^- fluxes in the two root zones may lead to different concentrations of NO_3^- and NH_4^+, these concentrations in the two root zones were analyzed. Nitrate and NH_4^+ concentrations were significantly reduced by 46 and 43%, respectively, in root zone II in comparison with those in zone I (Figure 2). The activity of NR was lower in root zone II than in root zone I (Figure 2). The activities of GS and GOGAT, however, showed no significant difference between root zones II and I (Figure 2).

Identification of known and novel miRNAs

High-throughput sequencing of root zones I and II yielded 11.55 million raw reads per library. After screening, out redundant reads 5,752,458 and 7,379,124 valid reads corresponded to 1,996,697 and 1,996,482 unique reads in the zones I and II libraries, respectively (Table S2). After removing low-quality sequences, 18- to 25-nt-long sequences were retained. The proportions of unique sRNAs with lengths from 18 to 25 nts are summarized in Figure 3a. No significant differences
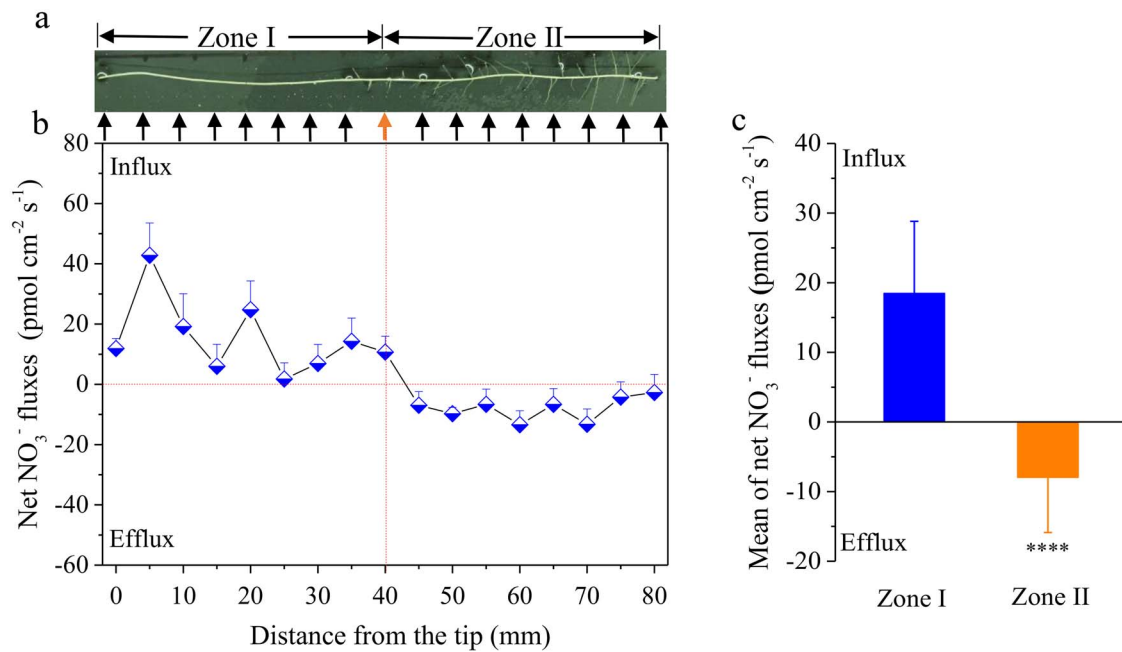
Figure 1. Different root zones (a), net NO_3^- fluxes (b) and the means of net NO_3^- fluxes (c) of *P. × canescens*. Data are presented as means ± SE (*n* = 6). (b) Each arrow indicates a measuring point along the root tip and the red arrow also indicates the border between root zones I and II. (c) Blue and orange bars indicate the mean values of net NO_3^- fluxes from zones I to II, respectively; positive and negative values correspond to net influxes and effluxes, respectively; the *P*-values from one-way ANOVA for the different root zones are indicated: ****$P < 0.0001$.
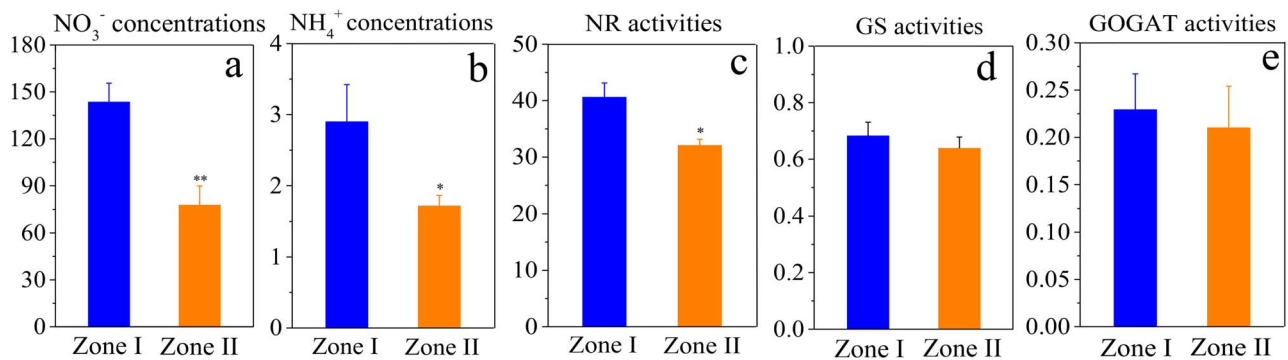

Figure 2. Concentrations of NO_3^- (µmol g^{-1} DW) and NH_4^+ (µmol g^{-1} DW), and activities of NR (nmol NO_3^- h^{-1} mg^{-1} protein), GS (µmol h^{-1} mg^{-1} protein) and GOGAT (nkat mg^{-1} protein) in two root zones of *P. × canescens*. The blue and orange bars indicate means ± SE (*n* = 6) of the data for the relevant parameters from zones I to II, respectively. *P* values from one-way ANOVA for the different root zones are indicated: *$P < 0.05$; **$P < 0.01$.

in the proportions of unique sRNAs were found between the root zone I and zone II libraries, and sRNAs of 24 nts were more common than those of other lengths in both libraries.

In total, 643 unique known miRNAs were identified in the root zones I and II libraries (Tables 1 and S4 available as Supplementary Data at *Tree Physiology* Online). These 643 miRNAs were derived from 569 miRNA precursors and belonged to 58 miRNA families (Table S3 available as Supplementary Data at *Tree Physiology* Online). Moreover, 70 pre-miRNAs, corresponding to 73 mature miRNAs, were identified as novel miRNA candidates (Table S5 available as Supplementary Data at *Tree Physiology* Online). In both libraries, miRNAs of 21 nts were more common than those of other lengths (Figure 3b).

Differentially expressed miRNAs

In total, 64 miRNAs, including 27 known miRNA families and 6 novel miRNAs, showed significantly differential expression (Figure 4, Table S6 available as Supplementary Data at *Tree Physiology* Online). About 41 upregulated and 23 downregulated miRNAs were identified in root zone II compared with root zone I (Figure 4, Table S6 available as Supplementary Data at *Tree Physiology* Online), and these results were validated by qRT-PCR analysis (Figure S1 available as Supplementary Data at *Tree Physiology* Online). Notably, miRNAs belonging to the same family frequently exhibited similar expression profiles. For example, the expression levels of nine miRNAs belonging to the
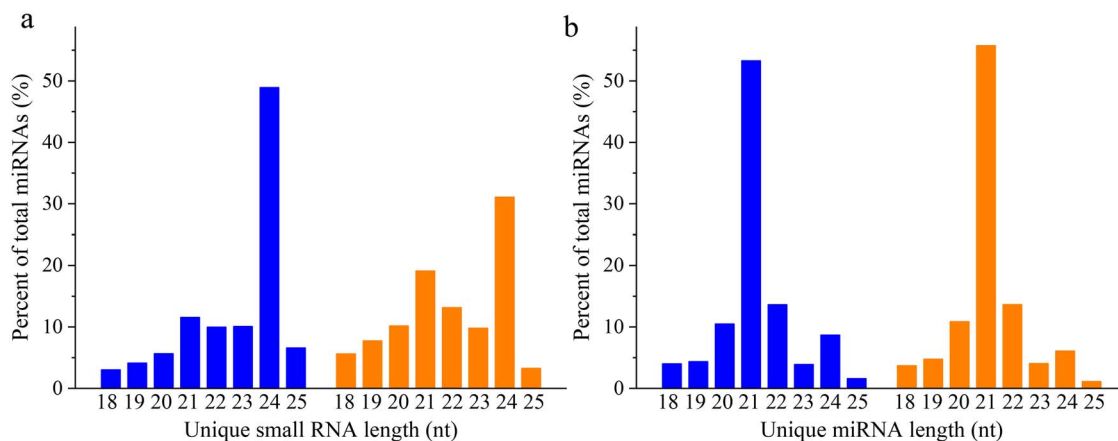
Figure 3. Lengths of unique sRNAs (a) and miRNAs (b) in two root zones of *P. × canescens*. The blue and orange bars indicate data from root zones I to II, respectively.

Table 1. The number of identified known and novel miRNAs in two root zones of *P. × canescens*.

Root zones	Known/novel miRNAs	Pre-miRNAs	Mature miRNAs
Zone I	Known	460	469
	Novel	37	39
Zone II	Known	480	492
	Novel	64	63
Total	Known	569	643
	Novel	70	73

miR171 family were increased, whereas those of four members of the miR8175 family and five members of the miR6300 family were significantly decreased in root zone II in comparison with zone I (Figure 4).

Prediction of miRNA targets

To further understand the roles of the 64 significantly differentially expressed miRNAs in *P. × canescens* roots, the targets of these miRNAs were predicted using TargetFinder (Table S7 available as Supplementary Data at *Tree Physiology* Online). In total, 576 targets were predicted based on these miRNAs (Table S7 available as Supplementary Data at *Tree Physiology* Online). These targets were assigned to functional categories using MapMan (Table S7 available as Supplementary Data at *Tree Physiology* Online). Enrichment in several functional categories, including transport, development, RNA regulation of transcription, stress and hormone metabolism, was observed (Table S7 available as Supplementary Data at *Tree Physiology* Online).

In particular, the targets of two significantly differentially expressed novel miRNAs associated with N transport, root development and N metabolism were predicted (Table 2). One target of downregulated PC-3p-61432_100 was predicted to be *ATP-binding cassette transporter subfamily G12* (*ABCG12*). The other

target of PC-3p-61432_100 was a *leucine-rich repeat transmembrane protein kinase*. Another target of upregulated PC-5p-35885_222 was a *G-type lectin S-receptor-like serine/threonine-protein kinase*. Four target genes of PC-5p-35885_222 encoded *serine-type endopeptidase/serine-type peptidases*.

Correlations between miRNAs and their targets

Among the 64 significantly differentially expressed miRNAs and their targets, 13 miRNA-target pairs were identified (Table 3). The expression levels of seven miRNA-target pairs exhibited negative correlations. These miRNA-target pairs included ptc-miR396g-5p/ptc-miR396f_L + 1R-1 and their target *growth-regulating factor 4* (*GRF4*), ptc-miR1515_L-1 and its target *snakin-2* (*SN2*), ptc-miR167e and its target *ethylene-responsive transcription factor LEP* (*LEP*), ptc-miR172b-5p and its target *peroxisomal (S)-2-hydroxy-acid oxidase GLO5-like*, and ptc-miR8175_1ss2AT/ptc-miR8175_L + 1_1ss3AT and their target *embryo defective 2016* (*EMB2016*) (Table 3). Conversely, the expression levels of the other six miRNA-target pairs exhibited positive correlations. These miRNA-target pairs included ptc-miR396g-5p/ptc-miR396f_L + 1R-1 and their target *trafficking protein particle complex subunit 2* (*TRAPPC2*)), ptc-miR169i-p5_3ss3GT20TC21GA and its target *indeterminate(ID)-domain 5* (*IDD5*), ptc-miR172k and its target *floral homeotic protein APETALA 2* (*AP2*), ptc-miR166c_2ss1TG20TC and its target *homeobox-leucine zipper protein REVOLUTA*, and ptc-miR482f_2ss8TC14AT and its target *inositol 2-dehydrogenase* (Table 3). The correlations between these miRNAs and their targets were validated by qRT-PCR (Figure 5).

Validation of miRNA-target pairs

To validate the miRNA-target pairs mentioned above, transient co-expression assays were carried out in *N. benthamiana* leaves for two randomly selected miRNA-target pairs, ptc-miR396f_L + 1R-1-*GRF4* and ptc-miR167e-*LEP*. The mRNA
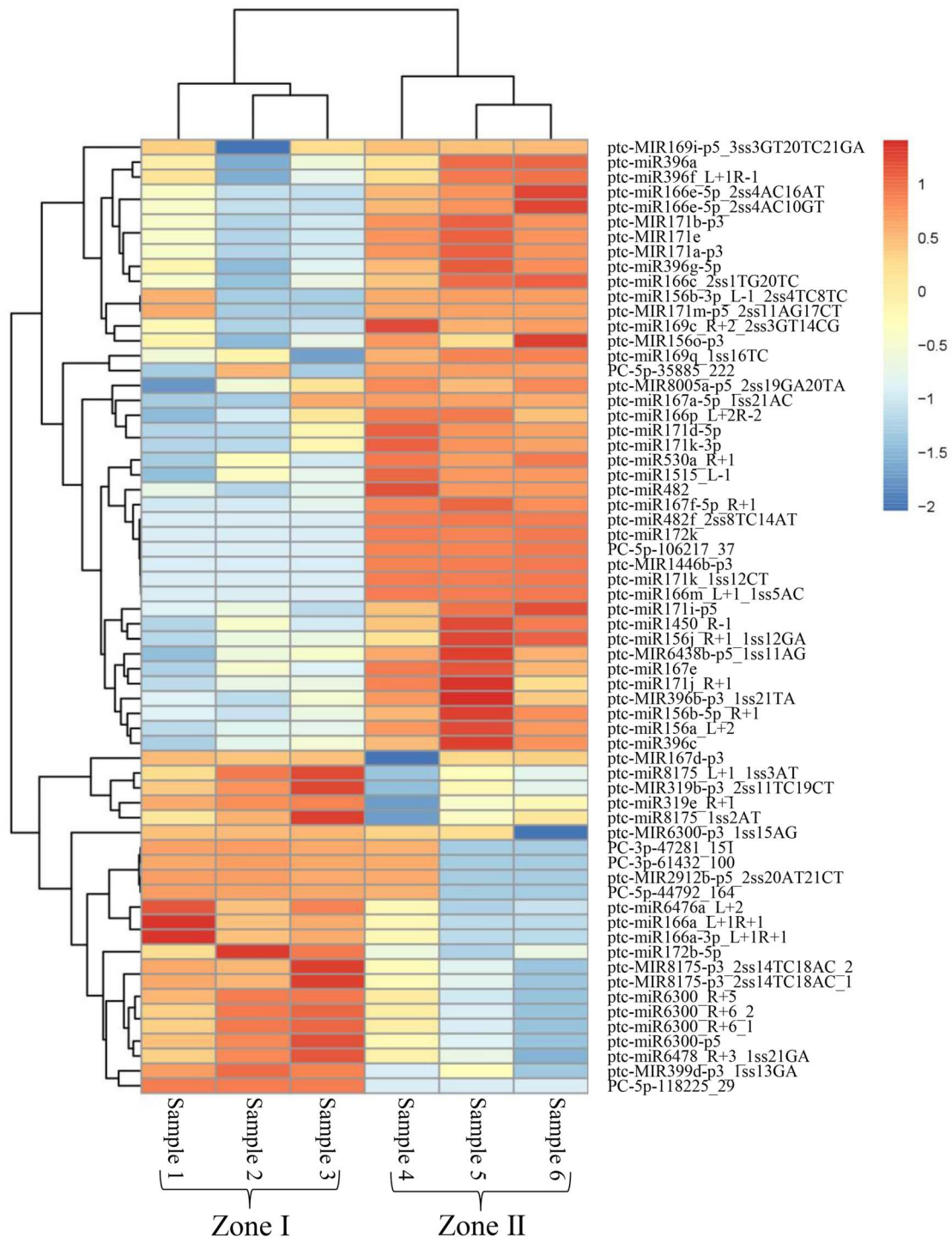
Figure 4. Significantly differentially expressed miRNAs in two root zones of *P.* × *canescens*. Red and blue indicate up- and down-regulation, respectively.

level of *GRF4* was significantly decreased when it was co-expressed with ptc-miR396f_L + 1R-1, and the transcript level of *LEP* was also significantly reduced when ptc-miR167e was co-expressed, in comparison with those of only the target genes *GRF4* and *LEP*, which were transiently expressed in *N. benthamiana* leaves (Figure 6). These results suggest that *GRF4* and *LEP* are the targets of ptc-miR396f_L + 1R-1 and ptc-miR167e, respectively.

Discussion

Nitrate uptake rates and assimilation were reduced in root zone II versus root zone I

Fine roots are composed of the root crown, meristem, elongation and maturation zones, which have different anatomical and functional characteristics, resulting in different capacities for NO_3^- uptake (Liu et al. 2013, Hawkins et al. 2014, Zhang
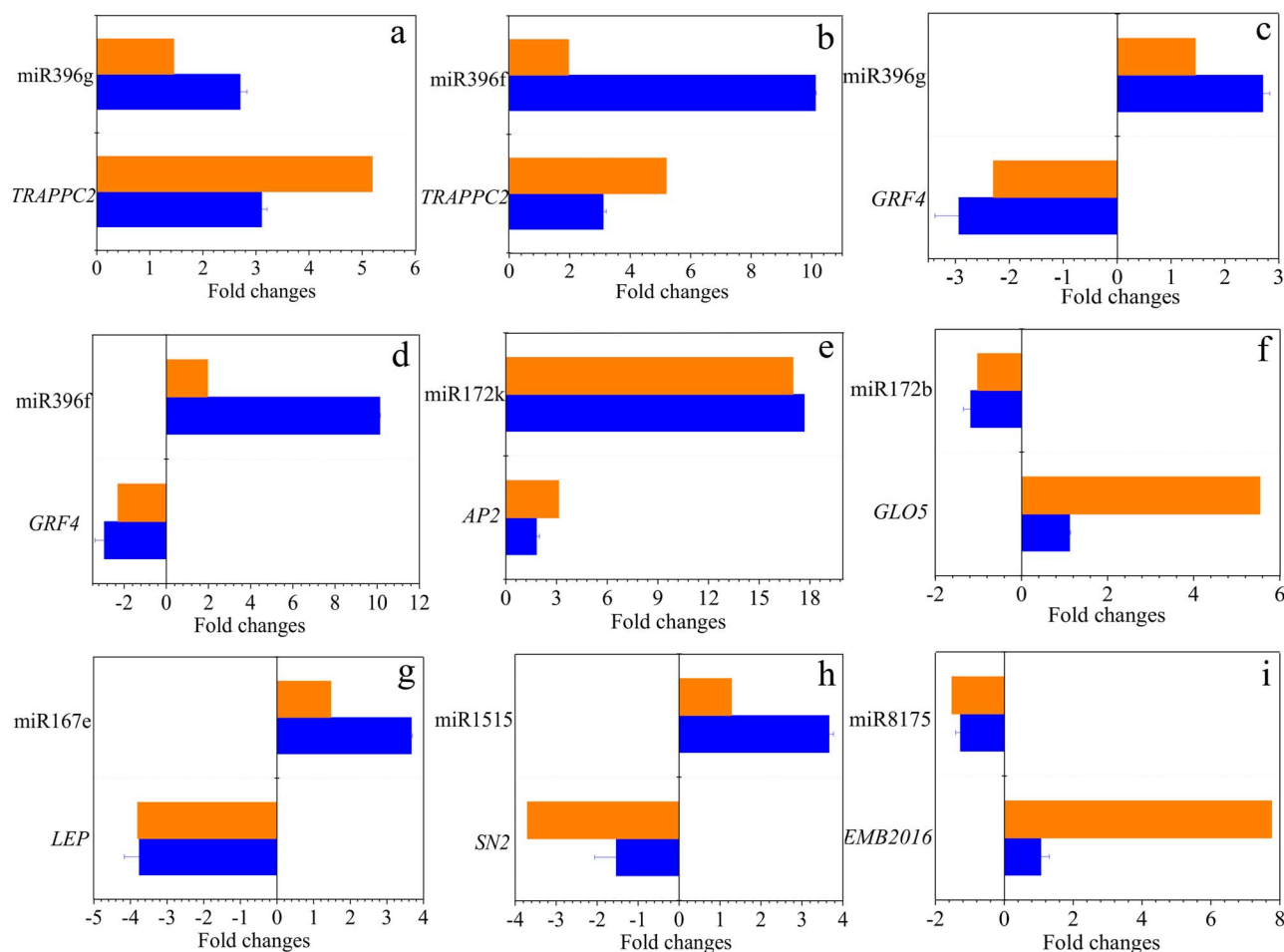
Figure 5. Validation of significantly differentially expressed miRNAs and their targets in two root zones of *P. × canescens*. The blue and orange bars indicate the data obtained by qRT-PCR and sRNA-seq, respectively.

et al. 2014). Different root zones of plants have distinct net NO_3^- fluxes (Sorgonà et al. 2010, Alber et al. 2012, Hawkins et al. 2014, Zhong et al. 2014, Lupini et al. 2016, Duan et al. 2018). For example, the position at a root of 30 mm from the tip displayed a significantly higher NO_3^- influx rate than did roots of 10 and 50 mm in maize under 50 µM KNO_3 conditions (Lupini et al. 2016). In *P. popularis*, the region 0–0.3 mm from the root tip displayed net NO_3^- efflux, though net NO_3^- influx was observed at 0.3–30 mm, and the maximal net uptake of NO_3^- occurred at 15 mm from the root tip under 100 µM NH_4NO_3 conditions (Luo et al. 2013b). In this study, the region at 0–40 mm from the root tip displayed net NO_3^- influxes, in contrast, net effluxes were observed at 40–80 mm, and the maximal net uptake occurred at 5 mm from the root tip. These results suggest that net NO_3^- influx or efflux varies spatially in different root zones of plants, possibly due to the different functional characteristics of different root zones (Luo et al. 2013*a*, 2013*b*, Zhong et al. 2014, Ruan et al. 2016).

In *P. × canescens*, NO_3^- uptake rates were reduced in root zone II with lateral roots in comparison with root zone I without

lateral roots (Figure S2 available as Supplementary Data at *Tree Physiology* Online), This finding is consistent with the results of previous studies in woody plants. Net NO_3^- fluxes were lower at 30–50 mm from the root tip than those at 0–30 mm in Douglas fir (*Pseudotsuga menziesii* Dode), Sitka spruce (*Picea sitchensis*) and Western red cedar (*Thuja plicata* Donn.) under 1500 µM NH_4NO_3 conditions (Hawkins et al. 2014). These results suggest that spatial variation in the uptake of NO_3^- in roots may be related to the occurrence of lateral roots at the base regions along the roots. Moreover, plants have evolved highly flexible and dynamic NO_3^- transport systems to acquire NO_3^-, leading to net NO_3^- influx or efflux in different root zones (Alber et al. 2012, Lupini et al. 2016, Duan et al. 2018). Thus, lower NO_3^- uptake rates in root zone II than root zone I of *P. × canescens* are probably associated to different expression patterns of NO_3^- transporter genes in both root zones (Figure S3 available as Supplementary Data at *Tree Physiology* Online).

Nitrate uptake rates in root zones may affect NO_3^- concentrations and activities of enzymes involved in NO_3^- assimilation (Deane-Drummond and Glass 1983, Teyker et al. 1988, Miller

Table 2. Selected novel miRNAs and their target genes.

miRNA IDs	Transcript IDs	Transcript annotations
PC-3p-61432_100	Potri.003G057300.1	ATP-binding cassette transporter, subfamily G, member 12, group WBC protein PpABCG12
	Potri.001G398500.1	Leucine-rich repeat transmembrane protein kinase
	Potri.002G242900.1	–
PC-5p-35885_222	Potri.014G135200.3	Serine-type endopeptidase/serine-type peptidase
	Potri.014G135200.1	Serine-type endopeptidase/serine-type peptidase
	Potri.008G201500.3	Ribonucleoside-diphosphate reductase small chain family protein
	Potri.014G135200.2	Serine-type endopeptidase/serine-type peptidase
	Potri.008G201500.2	Ribonucleoside-diphosphate reductase small chain family protein
	Potri.002G207200.1	Serine-type endopeptidase/serine-type peptidase
	Potri.013G098000.1	Animal HSPA9 nucleotide-binding domain protein
	Potri.004G026400.1	G-type lectin S-receptor-like serine/threonine-protein kinase CES101
	Potri.005G196100.1	–
	Potri.008G201500.1	Ribonucleoside-diphosphate reductase small chain family protein
	Potri.012G135000.1	Hypothetical protein

Table 3. Differentially expressed miRNAs and their targets in two root zones of $P. \times canescens$.

miRNA names	Up/Down	Target genes	Fold change	Annotation
ptc-miR396g-5p	Up	Potri.019G042300.1	−2.30	Growth-regulating factor 4 (GRF 4)
ptc-miR396f_L + 1R-1	Up	Potri.019G042300.1	−2.30	Growth-regulating factor 4 (GRF 4)
ptc-miR396g-5p	Up	Potri.003G183400.1	5.19	Trafficking protein particle complex (subunit 2 (TRAPPC2)
ptc-miR396f_L + 1R-1	Up	Potri.003G183400.1	5.19	Trafficking protein particle complex subunit 2 (TRAPPC2)
ptc-miR169i-p5_3ss3GT2OTC21GA	Up	Potri.008G142400.3	2.65	Indeterminate(ID)-domain 5 (IDD5)
ptc-miR172b-5p	Down	Potri.015G138500.5	5.54	Peroxisomal (S)-2-hydroxy-acid oxidase GLO5-like
ptc-miR172k	Up	Potri.008G045300.2	3.12	Floral homeotic protein APETALA 2 (AP2)
ptc-miR167e	Up	Potri.003G161000.1	−3.81	Ethylene-responsive transcription factor LEP
ptc-miR1515_L-1	Up	Potri.012G076700.1	−3.70	Snakin-2 (SN2)
ptc-miR166c_2ss1TG2OTC	Up	Potri.009G014500.4	2.17	Homeobox-leucine zipper protein REVOLUTA
ptc-miR482f_2ss8TC14AT	Up	Potri.003G078500.3	4.43	Inositol 2-dehydrogenase
ptc-miR8175_1ss2AT	Down	Potri.016G069100.3	7.77	EMB2016
ptc-miR8175_L + 1_1ss3AT	Down	Potri.016G069100.3	7.77	EMB2016

and Cramer 2005). In the present study, the NO_3^- uptake rates were reduced in root zone II versus root zone I, leading to lower concentrations of NO_3^- in root zone II. Similarly, the NO_3^- concentration is increased with enhanced NO_3^- uptake rate in strawberry roots under NO_3^- conditions (Darnell and Stutte 2001). These results indicate that the lower ability of root zone II to take up NO_3^- compared with root zone I can result in less amount of NO_3^- to be assimilated in zone II of $P. \times canescens$. Nitrate reductase is an inducible enzyme involved
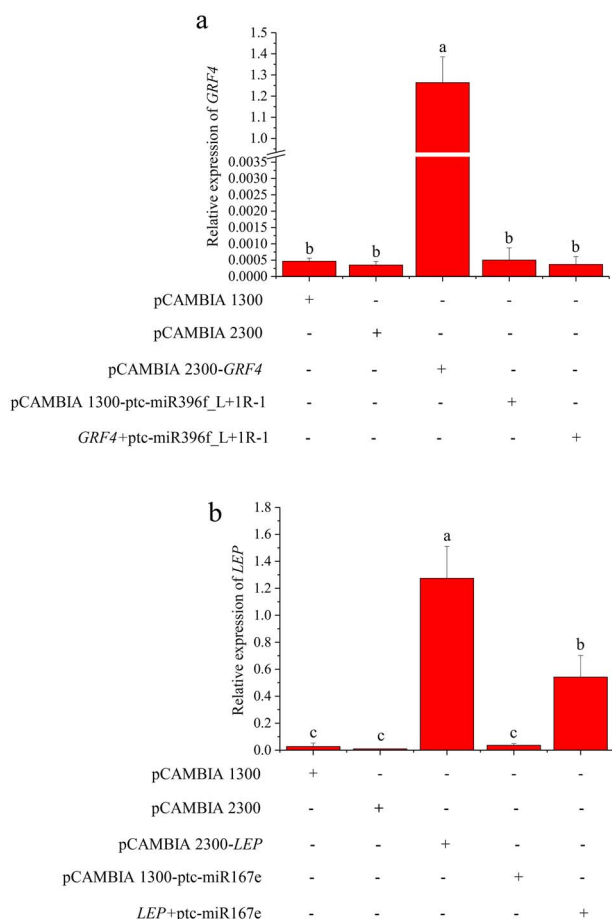
Figure 6. Validation of ptc-miR396f_L + 1R-1-*GRF4* (a) and ptc-miR167e-*LEP* (b) using transient co-expression assays in *N. benthamiana* leaves. pCAMBIA 1300 and pCAMBIA 2300 are two empty vectors. pCAMBIA 2300-*GRF4* (a) and pCAMBIA 2300-*LEP* (b) represent that only target genes were transferred to *N. benthamiana* leaves, respectively. pCAMBIA 1300-miR396f_L + 1R-1 (a) and pCAMBIA 1300-ptc-miR167e (b) represent that only miRNAs were transferred to *N. benthamiana* leaves, respectively. *GRF4* + miR396f_L + 1R-1 (a) and *LEP* + ptc-miR167 (b) represent that both the miRNA and its target were transferred to *N. benthamiana* leaves, respectively, and as a result the expression levels of the target genes were significantly decreased. The expression levels were quantified using qRT-PCR. Bars indicate means ± SE (*n* = 4). Different letters on the error bars indicate significant differences.

in NO_3^- assimilation. In line with lower NO_3^- concentrations in root zone II, the activity of NR was also lower in root zone II than in root zone I in *P. × canescens*.

miRNAs can regulate their targets involved in NO_3^- uptake and assimilation to slow down N physiological processes in root zone II versus root zone I

miRNAs are well-known endogenous regulatory factors that negatively regulate gene expression via complementary cleavage (Sunkar et al. 2012). By regulating target genes, miRNAs participate in NO_3^- uptake and assimilation (Gifford et al. 2008, Vidal et al. 2010, Gutierrez 2012, Vidal et al. 2013,

Yan et al. 2014, Li et al. 2016). In this study, two of the most interesting miRNA-target pairs were ptc-miR396g-5p-*GRF4* and ptc-miR396f_L + 1R-1-*GRF4*. In rice, *GRF4* can improve NH_4^+ and NO_3^- absorption efficiency (Li et al. 2018). *GRF4* promotes the transcript levels of NO_3^- transporters, such as *NRT1.1B* and *NRT2.3a*, and of genes encoding NO_3^- assimilation enzymes, such as nitrate reductase 1 (*NIA1*), *NIA3* and nitrite reductase 1 (*NiR1*), to regulate N metabolism (Li et al. 2018). Several genes involved in NO_3^- transport and assimilation were downregulated in root zone II compared with root zone I in *P. × canescens* (Figure S3 available as Supplementary Data at *Tree Physiology* Online), which is likely related to *GRF4* downregulation in root zone II, probably contributing to decreased NO_3^- uptake rates. These results indicate that ptc-miR396g-5p/ptc-miR396f_L + 1R-1 and their target *GRF4* might be participated in NO_3^- uptake and assimilation in the two root zones of *P. × canescens* by differentially regulating transcript levels of key genes involved in NO_3^- assimilation.

IDD10 can regulate the transcription of *ammonium transporter 1;2* (*AMT1;2*) and *glutamate dehydrogenase 2* (*GDH 2*) to participate in N metabolism, and IDD10-mutant rice roots are hypersensitive to exogenous NH_4^+ (Xuan et al. 2013). *IDD5* was homologous to *IDD10*, and it was the target gene of ptc-miR169i-p5_3ss3GT20TC21GA, belonging to the C2H2 zinc finger family (Table S8 available as Supplementary Data at *Tree Physiology* Online). It is probable that *IDD5* might regulate the expression of N assimilation genes to affect net NO_3^- fluxes in different root zones. Interestingly, the target gene of ptc-miR172b-5p is predicted to be *peroxisomal (S)-2-hydroxy-acid oxidase GLO5-like*, which also belongs to the C2H2 zinc finger family (Table S8 available as Supplementary Data at *Tree Physiology* Online). *AP2*, belonging to the APETALA2/ethylene-responsive element binding protein family (AP2/ERF), is a target of ptc-miR172k, and the target gene (encoding an ethylene-responsive element-binding family protein) of the ptc-miR167e also belongs to the AP2/ERF family (Table S8 available as Supplementary Data at *Tree Physiology* Online). Members of the AP2/ERF transcription factor family are participated in root development and response to N deficiency (He et al. 2016). These results suggest that several C2H2 zinc finger family and AP2/ERF members, which are targeted by different miRNAs, function as key regulators in the two root zones, resulting in lower NO_3^- uptake rates and assimilation in root zone II than in zone I of *P. × canescens*.

A few of the miRNAs, in response to root development and N availability, were differentially expressed in root zone II versus zone I of *P. × canescens*. miRNA171 family members can suppress primary root elongation and respond to N starvation in *A. thaliana* (Llave et al. 2002, Wang et al. 2010, Liang et al. 2012). SCARECROW, which is a target of miR171 family members, is important for early root meristem patterning and
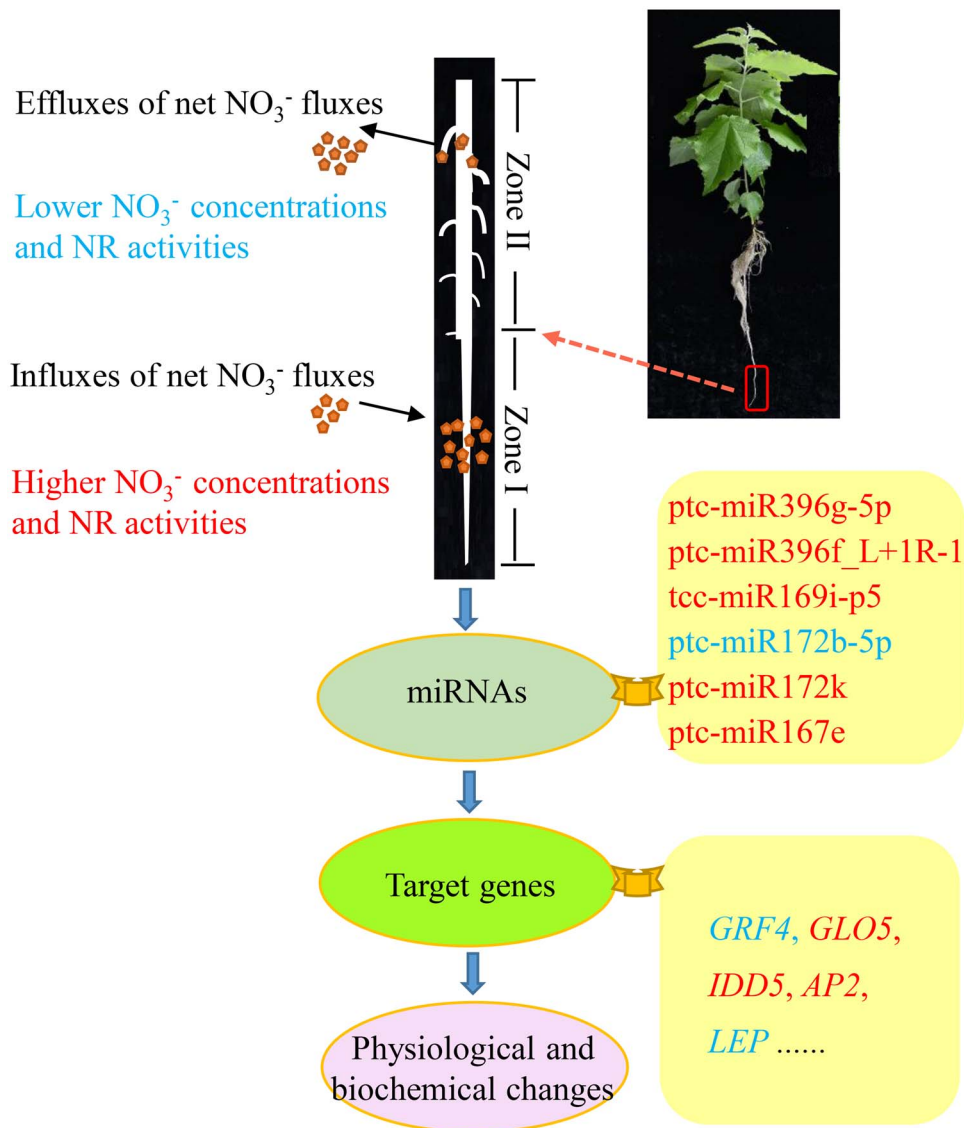
Figure 7. A simple model illustrates physiological and biochemical changes and miRNA regulation in root zone II in comparison with those in root zone I of *P. × canescens*.

maintenance (Stevens et al. 2018). Three targets of miR171, *Scarecrow-like protein 6* (*SCL6*)-*II*, *SCL6-III* and *SCL6-IV*, have been found to regulate the elongation of primary roots in *A. thaliana* (Llave et al. 2002, Wang et al. 2010, Liang et al. 2012). Interestingly, we found nine upregulated miR171 family members in root zone II in comparison with zone I in *P. × canescens*. In *A. thaliana*, miR8175 is responsive to the presence of 5 mM KNO_3 (Vidal et al. 2013). In this study, we found four downregulated miR8175 members in root zone II compared with root zone I. These results suggest that these miRNAs are likely participated in NO_3^- uptake and assimilation by changing root morphology and slowing down N physiological processes in root zone II versus root zone I. Further studies of these miRNA target genes will help in elucidating the NO_3^- uptake and assimilation processes between root zones I and II.

Conclusions

Based on the present results, a model of NO_3^- uptake and assimilation was proposed in the two root zones of *P. × canescens* (Figure 7). Root zone I (0–40 mm) displayed net NO_3^- influxes but root zone II (40–80 mm) net NO_3^- effluxes. Concentrations of NH_4^+ and NO_3^-, and the NR activity were lower in root zone II than in root zone I. In line with these physiological changes, 64 significantly differentially expressed miRNAs were identified and 576 target genes of these miRNAs were predicted. In particular, *GRF4*, a target of upregulated ptc-miR396g-5p and ptc-miR396f_L + 1R-1, was downregulated in root zone II in comparison with root zone I, probably contributing to lower NO_3^- uptake rates and assimilation in root zone II. Moreover, several miRNA-target pairs involved in N assimilation were identified in two root zones, which probably play important

roles in regulating NO_3^- uptake. These findings suggest that differentially expressed miRNA-target pairs play key roles in regulation of distinct NO_3^- uptake rates and assimilation in different root zones of poplars.

Supplementary Data

Supplementary Data for this article are available at *Tree Physiology* Online.

Acknowledgments

Funding

Conflict of interest

None declared.

Authors' contributions

J.Z. and Z.L. conceived the experiment, and J.Z., Y.L., W.S., S.D., and Z.L. performed the experimental and data analysis. J.Z. and Z.L. interpreted the experimental data and wrote the manuscript. All authors read and approved the final manuscript.

References

Alber A, Ehlting B, Ehlting J, Hawkins BJ, Rennenberg H (2012) Net NH_4^+ and NO_3^- flux, and expression of NH_4^+ and NO_3^- transporters in roots of *Picea glauca*. Trees 26:1403–1411.

Allen E, Xie Z, Gustafson AM, Carrington JC (2005) microRNA-directed phasing during trans-acting siRNA biogenesis in plants. Cell 121:207–221.

Cao D, Xu H, Zhao Y, Deng X, Liu Y, Soppe WJ, Lin J (2016) Transcriptome and degradome sequencing reveals dormancy mechanisms of *Cunninghamia lanceolata* seeds. Plant Physiol 172:2347–2362.

Colmer TD, Bloom AJ (1998) A comparison of NH_4^+ and NO_3^- net fluxes along roots of rice and maize. Plant Cell Environ 21:240–246.

Cruz C, H LS, MarEins-Loução (1995) Uptake regions of inorganic nitrogen in roots of carob seedlings. Physiol Plant 95:167–175.

Darnell RL, Stutte GW (2001) Nitrate concentration effects on NO_3^--N uptake and reduction, growth, and fruit yield in strawberry. J Am Soc Hortic Sci 126:560–563.

Deane-Drummond CE, Glass AD (1983) Short term studies of nitrate uptake into barley plants using ion-specific electrodes and $^{36}ClO_3^{-1}$: I. Control of net uptake by NO_3^{-1} efflux. Plant Physiol 73:100–104.

Dluzniewska P, Gessler A, Dietrich H, Schnitzler JP, Teuber M, Rennenberg H (2007) Nitrogen uptake and metabolism in *Populus × canescens* as affected by salinity. New Phytol 173:279–293.

Duan F, Giehl RFH, Geldner N, Salt DE, von Wiren N (2018) Root zone-specific localization of AMTs determines ammonium transport pathways and nitrogen allocation to shoots. PLoS Biol 16:e2006024.

Gifford ML, Dean A, Gutierrez RA, Coruzzi GM, Birnbaum KD (2008) Cell-specific nitrogen responses mediate developmental plasticity. Proc Natl Acad Sci USA 105:803–808.

Griffiths-Jones S, Saini HK, van Dongen S, Enright AJ (2008) miRBase: tools for microRNA genomics. Nucleic Acids Res 36:D154–D158.

Gutierrez RA (2012) Systems biology for enhanced plant nitrogen nutrition. Science 336:1673–1675.

Hawkins BJ, Robbins S, Porter RB (2014) Nitrogen uptake over entire root systems of tree seedlings. Tree Physiol 34:334–342.

He X, Ma H, Zhao X et al. (2016) Comparative RNA-Seq analysis reveals that regulatory network of maize root development controls the expression of genes in response to N stress. PLoS One 11:e0151697.

He XF, Fang YY, Feng L, Guo HS (2008) Characterization of conserved and novel microRNAs and their targets, including a TuMV-induced TIR-NBS-LRR class R gene-derived novel miRNA in Brassica. FEBS Lett 582:2445–2452.

Henriksen GH, Bloom AJ, Spanswick RM (1990) Measurement of net fluxes of ammonium and nitrate at the surface of barley roots using ion-selective microelectrodes. Plant Physiol 93:271–280.

Jia J, Zhou J, Shi W, Cao X, Luo J, Polle A, Luo ZB (2017) Comparative transcriptomic analysis reveals the roles of overlapping heat-/drought-responsive genes in poplars exposed to high temperature and drought. Sci Rep 7:43215.

Jiang L, Ball G, Hodgman C, Coules A, Zhao H, Lu C (2018) Analysis of gene regulatory networks of maize in response to nitrogen. Genes (Basel) 9:151.

Kant S (2018) Understanding nitrate uptake, signaling and remobilization for improving plant nitrogen use efficiency. Semin Cell Dev Biol 74:89–96.

Li H, Hu B, Wang W, Zhang Z, Liang Y, Gao X, Li P, Liu Y, Zhang L, Chu C (2016) Identification of microRNAs in rice root in response to nitrate and ammonium. J Genet Genomics 43:651–661.

Li S, Tian Y, Wu K et al. (2018) Modulating plant growth-metabolism coordination for sustainable agriculture. Nature 560:595–600.

Liang G, He H, Yu D (2012) Identification of nitrogen starvation-responsive microRNAs in *Arabidopsis thaliana*. PLoS One 7:e48951.

Liu Y, Lai N, Gao K, Chen F, Yuan L, Mi G (2013) Ammonium inhibits primary root growth by reducing the length of meristem and elongation zone and decreasing elemental expansion rate in the root apex in *Arabidopsis thaliana*. PLoS One 8:e61031.

Llave C, Xie Z, Kasschau KD, Carrington JC (2002) Cleavage of scarecrow-like mRNA targets directed by a class of *Arabidopsis* miRNA. Science 297:2053–2056.

Luo J, Li H, Liu T, Polle A, Peng C, Luo ZB (2013*a*) Nitrogen metabolism of two contrasting poplar species during acclimation to limiting nitrogen availability. J Exp Bot 64:4207–4224.

Luo J, Qin J, He F, Li H, Liu T, Polle A, Peng C, Luo ZB (2013*b*) Net fluxes of ammonium and nitrate in association with H$^+$ fluxes in fine roots of *Populus popularis*. Planta 237:919–931.

Lupini A, Mercati F, Araniti F, Miller AJ, Sunseri F, Abenavoli MR (2016) NAR2.1/NRT2.1 functional interaction with $NO_3^{(-)}$ and H$^{(+)}$ fluxes in high-affinity nitrate transport in maize root regions. Plant Physiol Biochem 102:107–114.

Miller AJ, Cramer MD (2005) Root nitrogen acquisition and assimilation. Plant Soil 274:1–36.

Miller AJ, Fan X, Orsel M, Smith SJ, Wells DM (2007) Nitrate transport and signaling. J Exp Bot 58:2297–2306.

Patterson K, Cakmak T, Cooper A, Lager I, Rasmusson AG, Escobar MA (2010) Distinct signaling pathways and transcriptome response

signatures differentiate ammonium- and nitrate-supplied plants. Plant Cell Environ 33:1486–1501.

Pertea M, Pertea GM, Antonescu CM, Chang TC, Mendell JT, Salzberg SL (2015) StringTie enables improved reconstruction of a transcriptome from RNA-seq reads. Nat Biotechnol 33:290–295.

Pfaffl MW, Horgan GW, Dempfle L (2002) Relative expression software tool (REST©) for group-wise comparison and statistical analysis of relative expression results in real-time PCR. Nucleic Acids Res 30: e36.

Qu CP, Xu ZR, Hu YB, Lu Y, Yang CJ, Sun GY, Liu GJ (2016) RNA-SEQ reveals transcriptional level changes of poplar roots in different forms of nitrogen treatments. Front Plant Sci 7:51.

Remans T, Nacry P, Pervent M, Filleur S, Diatloff E, Mounier E, Tillard P, Forde BG, Gojon A (2006) The *Arabidopsis* NRT1.1 transporter participates in the signaling pathway triggering root colonization of nitrate-rich patches. Proc Natl Acad Sci USA 103: 19206–19211.

Ren Y, Sun F, Hou J, Chen L, Zhang Y, Kang X, Wang Y (2015) Differential profiling analysis of miRNAs reveals a regulatory role in low N stress response of *Populus*. Funct Integr Genomics 15: 93–105.

Rennenberg H, Wildhagen H, Ehlting B (2010) Nitrogen nutrition of poplar trees. Plant Biol (Stuttg) 12:275–291.

Rewald B, Kunze ME, Godbold DL (2016) NH$_4$: NO$_3$ nutrition influence on biomass productivity and root respiration of poplar and willow clones. GCB Bioenergy 8:51–58.

Ruan L, Wei K, Wang L, Cheng H, Zhang F, Wu L, Bai P, Zhang C (2016) Characteristics of NH$_4^{(+)}$ and NO$_3^{(-)}$ fluxes in tea (*Camellia sinensis*) roots measured by scanning ion-selective electrode technique. Sci Rep 6:38370.

Ruan L, Wei K, Wang L, Cheng H, Wu L, Li H (2019) Characteristics of free amino acids (the quality chemical components of tea) under spatial heterogeneity of different nitrogen forms in tea (*Camellia sinensis*) plants. Molecules 24:415.

Selle A, Willmann M, Grunze N, Gessler A, Weiss M, Nehls U (2005) The high-affinity poplar ammonium importer PttAMT1.2 and its role in ectomycorrhizal symbiosis. New Phytol 168:697–706.

Sorgonà A, Cacco G, Di Dio L, Schmidt W, Perry PJ, Abenavoli MR (2010) Spatial and temporal patterns of net nitrate uptake regulation and kinetics along the tap root of *Citrus aurantium*. Acta Physiol Plant 32:683–693.

Sorgona A, Lupini A, Mercati F, Di Dio L, Sunseri F, Abenavoli MR (2011) Nitrate uptake along the maize primary root: an integrated physiological and molecular approach. Plant Cell Environ 34:1127–1140.

Stevens ME, Woeste KE, Pijut PM (2018) Localized gene expression changes during adventitious root formation in black walnut (*Juglans nigra* L.). Tree Physiol 38:877–894.

Sunkar R, Li YF, Jagadeeswaran G (2012) Functions of microRNAs in plant stress responses. Trends Plant Sci 17:196–203.

Tang G, Reinhart BJ, Bartel DP, Zamore PD (2003) A biochemical framework for RNA silencing in plants. Genes Dev 17:49–63.

Taylor AR, Bloom AJ (1998) Ammonium, nitrate, and proton fluxes along the maize root. Plant Cell Environ 21:1255–1263.

Teyker RH, Jackson WA, Volk RJ, Moll RH (1988) Exogenous NO$_{(3)}$ influx and endogenous NO$_{(3)}$ efflux by two maize (*Zea mays* L.) inbreds during nitrogen deprivation. Plant Physiol 86:778–781.

Vidal EA, Araus V, Lu C, Parry G, Green PJ, Coruzzi GM, Gutierrez RA (2010) Nitrate-responsive miR393/AFB3 regulatory module controls root system architecture in *Arabidopsis thaliana*. Proc Natl Acad Sci USA 107:4477–4482.

Vidal EA, Moyano TC, Krouk G, Katari MS, Tanurdzic M, McCombie WR, Coruzzi GM, Gutiérrez RA (2013) Integrated RNA-seq and sRNA-seq analysis identifies novel nitrate-responsive genes in *Arabidopsis thaliana* roots. BMC Genomics 14:701.

Wang L, Mai YX, Zhang YC, Luo Q, Yang HQ (2010) MicroRNA171c-targeted *SCL6-II*, *SCL6-III*, and *SCL6-IV* genes regulate shoot branching in *Arabidopsis*. Mol Plant 3:794–806.

Wu HJ, Wang ZM, Wang M, Wang XJ (2013) Widespread long noncoding RNAs as endogenous target mimics for microRNAs in plants. Plant Physiol 161:1875–1884.

Xu Y, Sun T, Yin L-P (2006) Application of non-invasive microsensing system to simultaneously measure both H and O$_2^-$ fluxes. J Integr Plant Biol 48:823–831.

Xuan YH, Priatama RA, Huang J et al. (2013) Indeterminate domain 10 regulates ammonium-mediated gene expression in rice roots. New Phytol 197:791–804.

Yan Y, Wang H, Hamera S, Chen X, Fang R (2014) miR444a has multiple functions in the rice nitrate-signaling pathway. Plant J 78: 44–55.

Yu C, Chen Y, Cao Y et al. (2018) Overexpression of miR169o, an overlapping microRNA in response to both nitrogen limitation and bacterial infection, promotes nitrogen use efficiency and susceptibility to bacterial blight in rice. Plant Cell Physiol 59:1234–1247.

Zhang C, Meng S, Li Y, Zhao Z (2014) Net NH$_4^+$ and NO$_3^-$ fluxes, and expression of NH$_4^+$ and NO$_3^-$ transporter genes in roots of *Populus simonii* after acclimation to moderate salinity. Trees 28:1813–1821.

Zhang C, Meng S, Li Y, Su L, Zhao Z (2016) Nitrogen uptake and allocation in *Populus simonii* in different seasons supplied with isotopically labeled ammonium or nitrate. Trees 30:2011–2018.

Zhong Y, Yan W, Chen J, Shangguan Z (2014) Net ammonium and nitrate fluxes in wheat roots under different environmental conditions as assessed by scanning ion-selective electrode technique. Sci Rep 4:7223.

Zhou J, Liu M, Jiang J, Qiao G, Lin S, Li H, Xie L, Zhuo R (2012) Expression profile of miRNAs in *Populus cathayana* L. and *Salix matsudana* Koidz under salt stress. Mol Biol Rep 39:8645–8654.

Zuluaga DL, De Paola D, Janni M, Curci PL, Sonnante G (2017) Durum wheat miRNAs in response to nitrogen starvation at the grain filling stage. PLoS One 12:e0183253.